

Magneto-Gyrotropic Photogalvanic Effect in Semiconductor Quantum Wells

V.V. Bel'kov^{1,2}, S.D. Ganichev^{1,2}, Petra Schneider¹, S. Gölzberger¹,

E.L. Ivchenko², S.A. Tarasenko², W. Wegscheider¹, D. Weiss¹, W. Prettl¹

¹Fakultät Physik, University of Regensburg, 93040, Regensburg, Germany and

²A.F. Ioffe Physico-Technical Institute,

Russian Academy of Sciences, 194021 St. Petersburg, Russia

Abstract

We investigate both experimentally and theoretically, the magneto-gyrotropic photogalvanic effect in zinc-blende based quantum wells with C_{2v} point-group symmetry using optical excitation in the terahertz frequency range. The investigated frequencies cause intra-subband but no inter-band and inter-subband transitions. While at normal incidence the photocurrent vanishes at zero magnetic field, it is shown that an in-plane magnetic field generates photocurrents both for polarized and unpolarized excitation. In general the spin-galvanic effect, caused by circularly polarized light, and the magneto-gyrotropic effect, caused by unpolarized excitation, is superimposed. It is shown that in the case of two specific geometries both effects are separable.

PACS numbers: 73.21.Fg, 72.25.Fe, 78.67.De, 73.63.Hs

INTRODUCTION

The photogalvanic effect (PGE), predicted independently by [1, 2] for bulk semiconductors, is characteristic for gyrotropic materials and was recently intensively studied, both theoretically and experimentally, in zinc-blende and diamond-lattice quantum well (QW) structures [3, 4]. In such systems a photocurrent flows under illumination with circularly polarized light which changes its direction if the helicity of the circular polarization is reversed. However, in the presence of a magnetic field a photocurrent can flow even if the light is unpolarized [1, 5]. This will be denoted as magneto-gyrotropic PGE below. The effect is due to the fact that the gyrotropic point-group symmetry makes no difference between components of polar and axial vectors and therefore feature currents $j \propto IB$ with I the light intensity and B the applied magnetic field. Here, the proportionality constant is an invariant.

The magneto-gyrotropic PGE occurring under linearly polarized irradiation in an applied magnetic field has been studied theoretically in bulk crystals and nanostructures [5, 6, 7, 8, 9]. Experimentally the effect was observed in QW structures [10, 11, 12], because the point groups D_{2d} and C_{2v} of (001)-grown symmetrical and asymmetrical QWs belong to gyrotropic classes. So far the magneto-gyrotropic photocurrent has been observed for direct optical transitions. A photocurrent caused by transitions between spin branches of the electron subband splitted due to the Rashba effect has been measured in a GaSb/InAs single QW structure (wavelength $\lambda = 385$ nm or $\hbar\omega = 3.2$ meV) [10]. A magnetic field induced photocurrent due to direct inter-band transitions has also been observed in GaAs/AlGaAs QWs in the spectral range $0.7 \mu\text{m} < \lambda < 1.4 \mu\text{m}$ and was attributed to the magnetic field induced spin-independent asymmetry of the electron dispersion in an asymmetric heterostructure [7, 11, 12]. Here we report on the observation of the magneto-gyrotropic photocurrent in n-doped InAs QWs under intra-subband absorption (indirect Drude-like transitions) of linearly and circularly polarized far-infrared radiation ($\lambda = 148$ μm and $\theta = 90^\circ$). The experimental results show that, in the samples under study, the magneto-gyrotropic photocurrent has a spin-related nature.

METHODS

The experiments are carried out on (001)-oriented n-type InAs/Al_{0.3}Ga_{0.7}Sb heterostructures having C_{2v} point symmetry. Single QWs of 15 nm width with free carrier densities of about $1.3 \times 10^{12} \text{ cm}^{-2}$ and mobility $2 \times 10^4 \text{ cm}^2/(\text{Vs})$ (data are obtained at room temperature) were grown by molecular-beam epitaxy. Several samples of the same batch were investigated at room temperature yielding the same results. The samples have two pairs of ohmic contacts at the corners corresponding to the Γ 001 directions, $x \parallel [100]$ and $y \parallel [010]$, and two additional pairs of contacts centered along opposite sample edges with connecting lines along $x^0 \parallel [110]$ and $y^0 \parallel [110]$ (see insets in Figs. 1–4). An external magnetic field B up to 1 T was applied parallel to the interface plane.

A pulsed optically pumped far-infrared laser was used for optical excitation [13]. With NH_3 as active gas 40 ns pulses with about 10 kW power have been obtained at the wavelengths 148 μm and 90 μm . The far-infrared radiation induces free carrier absorption (Drude-like) in the lowest conduction subband ϵ_1 because the photon energies are smaller than the subband separation and much larger than the k -linear spin splitting. The samples were irradiated along the growth direction by linearly or circularly polarized radiation. In all experiments the electric field vector of linearly polarized radiation was oriented perpendicularly to the magnetic field direction. Circular polarization was obtained by using a crystalline quartz $\lambda/4$ plate. The helicity P_{circ} of the incident light was varied according to $P_{\text{circ}} = \sin 2\theta$, where θ is the angle between the initial plane of linear polarization and the optical axis of the $\lambda/4$ plate. P_{circ} is equal to -1 for left-handed circularly polarized light

and $+1$ for right-handed polarization $+$. The photocurrent j was measured at room temperature in unbiased structures via the voltage drop across a 50 Ω load resistor in a closed circuit configuration.

EXPERIMENTAL RESULTS

By irradiating the QWs with normal incident linearly polarized light (see inset in Fig. 1) a fast photocurrent signal has been observed after applying an in-plane magnetic field. The signal follows the temporal structure of the laser pulse intensity, and the polarity of the current changes upon reversal of the applied magnetic field. The results obtained for

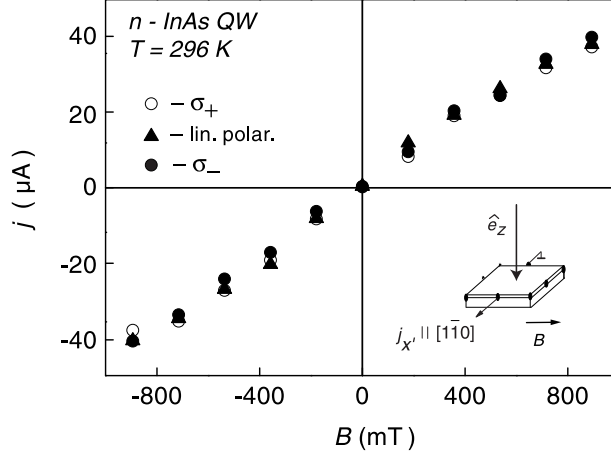


FIG. 1: Magnetic-field dependence of the photocurrent measured in InAs (001)-grown QWs at room temperature with magnetic field B parallel to $[110]$ direction. Optical excitation of 10 kW power at normal incidence was applied at wavelength $\lambda = 148$ nm with linear, right-handed circular ($+$), and left-handed circular ($-$) polarization. The current is measured normal to B . The inset shows the geometry of the experiment.

$\lambda = 90$ nm and for $\lambda = 148$ nm are qualitatively the same and differ only by a factor. Therefore below we present only data obtained for radiation with $\lambda = 148$ nm. For B aligned along a $[110]$ axis only a transverse effect, i.e. current flow in the direction perpendicular to the applied magnetic field, was detected (see triangles in Figs. 1 and 2). For another experimental configuration, $B \parallel [100]$, both longitudinal and transverse currents were observed, depicted in Fig. 3. In the absence of a magnetic field the signals vanish for all directions. This is the case for linear as well as circular polarization.

A magnetic field induced current has also been observed upon excitation with circularly polarized radiation. However, the orientation of the current with respect to the direction of the magnetic field and crystallographic axes is completely different. While for $B \parallel [110]$ absorption of linearly polarized light results in a photocurrent perpendicular to the magnetic field direction only, the excitation by circularly polarized radiation yields a current in both directions, normal and parallel to the magnetic field (Figs. 1 and 2). The current component normal to the magnetic field, applied along $y^0 \parallel [110]$, is independent of the radiation helicity and coincides with that induced by linearly polarized radiation (Fig. 1), say j_x^0 / IB_{y^0} where I is the intensity of the radiation. This observation indicates that the origin of this current is the same for both linearly and circularly polarized radiation. In contrast, the current

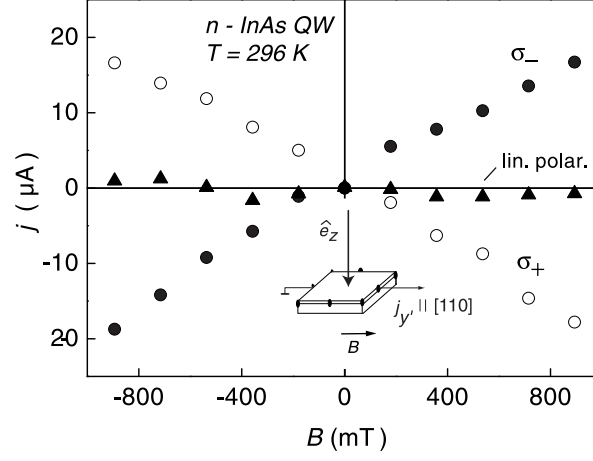


FIG. 2: Magnetic field dependence of the photocurrent measured with magnetic field B parallel to $[110]$ direction. Optical excitation at normal incidence was applied at wavelength $\lambda = 148$ nm with linear, right-handed circular ($+$), and left-handed circular (\circ) polarization. The current is measured parallel to B . The inset shows the geometry of the experiment.

along the magnetic field direction changes its sign upon changing the helicity from right- to left-handed and vanishes for linearly polarized radiation: $j_y^0 / IB_y^0 P_{\text{circ}}$ (see Fig. 2). This current has been observed previously [14] and is caused by the spin-galvanic effect due to optical orientation of carriers and the Larmor precession of electron spins.

If the magnetic field is applied along one of the cubic axes, say $B \parallel x$, the current generated by irradiation with helicity P_{circ} may be described by the empirical formula

$$j_i = (a_i + b_i P_{\text{circ}}) B_x I \quad (i = x, y) \quad (1)$$

and can be detected for both directions $x \parallel [100]$ and $y \parallel [010]$ (see Fig. 4). In this equation a_i and b_i are constants of the same order of magnitude. The helicity dependent component of the current determined by b_i is caused in this geometry by the spin-galvanic effect superimposed on a helicity independent contribution given by a_i .

PHENOMENOLOGY

In the linear approximation in the magnetic field strength B the magnetic field induced photogalvanic effect is phenomenologically given by

$$\mathbf{j} = \mathbf{B} \times \mathbf{E} + \mathbf{E}^2 \mathbf{g} + \mathbf{B} \times \mathbf{E}^2 \mathbf{P}_{\text{circ}}; \quad (2)$$

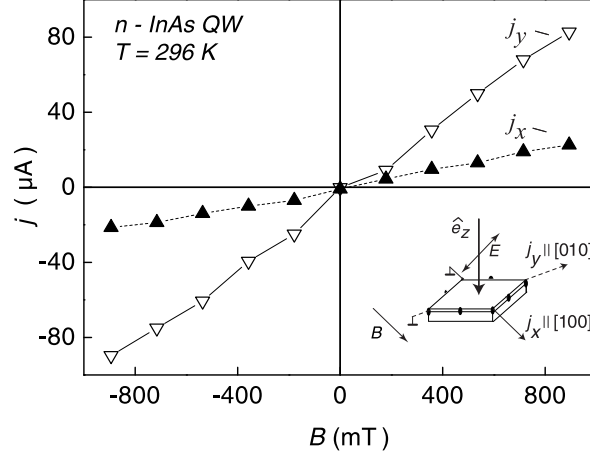


FIG . 3: Magnetic field dependence of the photocurrent measured with magnetic field B parallel to $[100]$ direction. Optical excitation at normal incidence was applied at wavelength $\lambda = 148$ nm with linear polarization. The current is measured parallel (j_x) and normal (j_y) to B . The inset shows the geometry of the experiment.

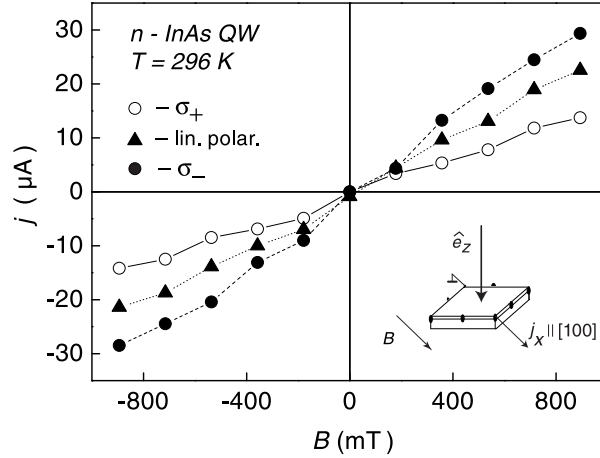


FIG . 4: Magnetic field dependence of the photocurrent measured with magnetic field B parallel to $[100]$ direction. Optical excitation at normal incidence was applied at wavelength $\lambda = 148$ nm with linear, right-handed circular (σ_+), and left-handed circular (σ_-) polarization. The current is measured parallel to B . The inset shows the geometry of the experiment.

where the first term on the right hand side gives the magneto-gyrotropic photogalvanic effect and the second term is the magnetic field induced spin-galvanic effect. In this equation, E is the electric field of the radiation with $E = E_0 e$, where E_0 is the real amplitude of the field and e denotes a complex polarization vector of unit length, $e \cdot e = 1$. $\nabla \times E^2 g$ is the

symmetrized product of the electric field with its complex conjugate

$$\mathbf{f} \cdot \mathbf{E} \mathbf{E}^* \mathbf{g} = \frac{1}{2} (\mathbf{E} \cdot \mathbf{E}^* + \mathbf{E} \cdot \mathbf{E}^*) : \quad (3)$$

The vector $\hat{\mathbf{e}}$ is the unit vector pointing in the direction of light propagation. The fourth rank tensor \mathbf{f} is symmetric in the last two indices. It is a pseudo-tensor whereas \mathbf{g} is a regular third rank tensor. While the second term on the right hand side of Eq. (2) requires circularly polarized radiation the first term may be non-zero even for unpolarized radiation.

In the following we consider (001)-oriented quantum wells based on III-V compounds. The symmetry of these quantum wells may belong to the point groups D_{2d} or C_{2v} depending, respectively, on equivalence or non-equivalence of the QW interfaces. The present experiments have been carried out on C_{2v} structures and, therefore, we will discuss this symmetry only.

In order to describe the experiments it is convenient to use both Cartesian coordinate systems introduced above. In the coordinate system $x^0 \parallel [110]$, $y^0 \parallel [\bar{1}10]$, $z \parallel [001]$, the in-plane axes lie in the crystallographic planes (110) and ($\bar{1}10$) which are the mirror reflection planes containing the two-fold axes of C_{2v} . In this coordinate system Eq. (2) can be reduced to

$$\begin{aligned} j_x^0 &= S_1 B_{y^0} I + S_2 B_{y^0} j_x^0 j_y^0 + j_x^0 j_y^0 I + S_3 B_{x^0} (e_x^0 e_{y^0} + e_{y^0} e_{x^0}) I + S_4 B_{x^0} IP_{\text{circ}}; \\ j_y^0 &= S_1^0 B_{x^0} I + S_2^0 B_{x^0} j_x^0 j_y^0 + j_x^0 j_y^0 I + S_3^0 B_{y^0} (e_x^0 e_{y^0} + e_{y^0} e_{x^0}) I + S_4^0 B_{y^0} IP_{\text{circ}}; \end{aligned} \quad (4)$$

In the crystallographic directions $x \parallel [100]$; $y \parallel [010]$, Eqs. (4) are rewritten as

$$\begin{aligned} j_x &= S_1^+ B_x I + S_1^- B_y I + (S_2^+ B_x + S_2^- B_y) (e_x e_y + e_y e_x) I \\ &+ (S_3^+ B_x - S_3^- B_y) j_x j_y + j_x j_y I + (S_4^+ B_x - S_4^- B_y) IP_{\text{circ}}; \\ j_y &= -S_1^- B_x I - S_1^+ B_y I + (S_2^- B_x + S_2^+ B_y) (e_x e_y + e_y e_x) I \\ &+ (-S_3^- B_x + S_3^+ B_y) j_x j_y + j_x j_y I + (-S_4^- B_x + S_4^+ B_y) IP_{\text{circ}}; \end{aligned} \quad (5)$$

where $S_l = (S_l - S_l^0)/2$ ($l = 1 \dots 4$). In these equations we set for the intensity $I = E_0^2$. The parameters S_1 to S_4 , S_1^0 to S_4^0 and S_1^- to S_4^- expressed by the non-zero elements of the tensors \mathbf{f} and \mathbf{g} allowed in C_{2v} symmetry are given in Table I and Table II, respectively. Equations (4) show that the first terms on the right hand side (parameters S_1, S_1^0) yield a

$S_1 = \frac{1}{2} (x^0 y^0 x^0 x^0 + x^0 y^0 y^0 y^0)$	$S_1^0 = \frac{1}{2} (y^0 x^0 x^0 x^0 + y^0 x^0 y^0 y^0)$
$S_2 = \frac{1}{2} (x^0 y^0 x^0 x^0 - x^0 y^0 y^0 y^0)$	$S_2^0 = \frac{1}{2} (y^0 x^0 x^0 x^0 - y^0 x^0 y^0 y^0)$
$S_3 = x^0 x^0 x^0 y^0 = x^0 x^0 y^0 x^0$	$S_3^0 = y^0 y^0 x^0 y^0 = y^0 y^0 y^0 x^0$
$S_4 = x^0 x^0 z$	$S_4^0 = y^0 y^0 z$

TABLE I: Definition of the parameters S_i and S_i^0 ($i = 1::4$) in Eqs. (4) in terms of non-zero components of the tensors χ_{ijkl} and χ_{ijkl}^0 for coordinates $x^0 \parallel [110]$, $y^0 \parallel [1\bar{1}0]$ and $z \parallel [001]$. C_{2v} symmetry and normal incidence of radiation along z is assumed.

current in the plane of the quantum well which is proportional to the intensity I and independent of the state of radiation polarization. This current is induced even for unpolarized radiation. In the case of the second and third terms linear polarization is needed in order to give a photocurrent. The photocurrent assumes a maximum for light polarized along x^0 or y^0 in the case of the second terms described by the parameters $S_2; S_2^0$ or along the bisector of x^0 and y^0 for the third terms proportional to $S_3; S_3^0$.

Thus, these terms do not contribute to the current if the radiation is circularly polarized. The last terms in Eqs. (4) describe a current proportional to the helicity of radiation being maximum for left- or right-handed circular polarization and changing sign when the helicity P_{circ} is switched from $+1$ to -1 . At normal incidence of radiation in all cases a magnetic field in the plane of the quantum well is required to obtain a current. At zero magnetic field no current is allowed at normal incidence of radiation in the present C_{2v} point group symmetry case and, in fact, it does not occur in experiment. The relations between polarization and magnetic field after Eqs. (4) and Eqs. (5) are summarized in Table III.

COMPARISON TO EXPERIMENTAL RESULTS

Now we analyze the phenomenological Eqs. (4) with respect to experiments. Three magnetic field orientations were applied, namely, $B \parallel y^0$, $B \parallel x^0$, and $B \parallel x$. Note that due to C_{2v} point group symmetry the geometry $B = (B; 0; 0) \parallel x$ is same to that for $B = (0; B; 0) \parallel y$, however, $B \parallel x^0$ and $B \parallel y^0$ are not equivalent. We discuss the electric current parallel and normal to the magnetic field in each case for three states of polarization:

$S_1^+ = \frac{1}{2} (\chi_{xxxx} + \chi_{xyxy})$ $= \frac{1}{2} (\chi_{yyxx} + \chi_{yyyy})$	$S_1 = \frac{1}{2} (\chi_{yxxx} + \chi_{xyyy})$ $= \frac{1}{2} (\chi_{yxxx} + \chi_{xyyy})$
$S_2^+ = \chi_{yyxy} = \chi_{yyyx}$ $= \chi_{xxxy} = \chi_{xxyx}$	$S_2 = \chi_{yxxy} = \chi_{yxyx}$ $= \chi_{xyxy} = \chi_{xyyx}$
$S_3^+ = \frac{1}{2} (\chi_{xxxx} - \chi_{xyxy})$ $= \frac{1}{2} (\chi_{yyxx} - \chi_{yyyy})$	$S_3 = \frac{1}{2} (\chi_{yxxx} - \chi_{xyyy})$ $= \frac{1}{2} (\chi_{yxxx} - \chi_{xyyy})$
$S_4^+ = \chi_{xxz} = \chi_{yyz}$	$S_4 = \chi_{xyz} = \chi_{yxz}$

TABLE II: Definition of the parameters S_i and S_i^0 ($i = 1::4$) in Eqs. (4) in terms of non-zero components of the tensors χ and χ^0 for coordinates x k [100], y k [010] and z k [001]. C_{2v} symmetry and normal incidence of radiation along z is assumed.

linear as well as left- and right-handed circular. In the experiments with linear polarized radiation the electric field vector is always oriented normally to B .

B k y^0 (Figs. 1 and 2):

In this configuration we find that strength and sign of the current measured in the direction normal to the magnetic field, x^0 , is the same for all three states of polarization (for linear polarization in this case $e_{x^0} \neq 0$, $e_{y^0} = 0$) as shown in Fig. 1. This allows us to conclude that the current in this geometry in our samples is dominated by the first term in Eqs. (4), $S_1 \neq 0$, while the second term is negligible, $S_2 = 0$. Thus, the observed magneto-gyrotropic effect is represented by a polarization-independent magnetic field induced photocurrent. The current along y^0 appears also, but for circular polarization only. It has the same magnitude for right- and left-handed circular polarization but changes sign if the helicity is switched from $+$ to $-$ and vanishes for linear polarization (see Fig. 2). This is due to the spin-galvanic effect described by the last term in Eqs. (2) and (4).

$B \parallel k \parallel x^0$:

Qualitatively we have the same situation as described above if we exchange x^0 and y^0 . The current densities, however, differ quantitatively. The magnitude of the photocurrent parallel to the magnetic field and caused by circularly polarized radiation is smaller than that in the above case $B \parallel k \parallel y^0$. The helicity independent and perpendicular to B current is, in contrast, also different, but it exceeds that in the previous configuration. This difference in photocurrents is due to the fact that for C_{2v} point symmetry the axes $[110]$ and $[\bar{1}\bar{1}0]$ are non-equivalent which is taken into account in Eqs. (4) by introducing independent parameters S_i and S_i^0 ($i = 1 :: 4$).

$B \parallel k \parallel x$ or $B \parallel k \parallel y$ (Figs. 3 and 4):

For an orientation of the magnetic field parallel to one of the two in-plane $h100i$ axes of the material we find for linearly polarized radiation current components not only perpendicular but, in contrast to the previous magnetic field orientations, also parallel to B as displayed in Fig. 3. For circularly polarized radiation we observe also the spin-galvanic current at contact pairs with connecting lines parallel and normal to the magnetic field. The spin-galvanic effect manifests itself by a difference of the strength of the current for left- and right-handed circular polarization. The spin-galvanic current is superimposed on the helicity independent magneto-gyrotropic current (Fig. 4).

M I C R O S C O P I C M O D E L

In general, the observed magneto-gyrotropic PGE described by the parameters $S_1; S_1^0$ in Eqs. (4) can be attributed to three possible mechanisms, two of them being spin-dependent and one spin-independent or diamagnetic. Here, we briefly characterize all, present qualitative estimations for each and discuss which mechanism is most likely responsible for the magneto-gyrotropic photocurrent observed in the samples under study. In the first mechanism the electric current appears due to an asymmetry of spin-dependent spin-conserving energy relaxation processes in a system of hot carriers heated by free carrier absorption [5]. Due to the Zeeman spin splitting of electron spin states in the magnetic field, say $B \parallel k \parallel x$, the difference in population of the spin branches $s_x = \pm 1/2$ is given by the ratio $g_B B_x = E$, where

		magneto-gyrotropic effect			SGE
		1 st term	2 nd term	3 rd term	4 th term
B_{kx^0}	$j_{x^0}=I$	0	0	$S_3 B_{x^0} e_{x^0} e_{y^0} + e_{y^0} e_{x^0}$	$S_4 B_{x^0} P_{\text{circ}}$
	$j_{y^0}=I$	$S_1^0 B_{x^0}$	$S_2^0 B_{x^0} \hat{p}_{x^0}^2 - \hat{p}_{y^0}^2$	0	0
B_{ky^0}	$j_{x^0}=I$	$S_1 B_{y^0}$	$S_2 B_{y^0} \hat{p}_{x^0}^2 - \hat{p}_{y^0}^2$	0	0
	$j_{y^0}=I$	0	0	$S_3^0 B_{y^0} e_{x^0} e_{y^0} + e_{y^0} e_{x^0}$	$S_4^0 B_{y^0} P_{\text{circ}}$
B_{kx}	$j_x=I$	$S_1^+ B_x$	$S_2^+ B_x e_x e_y + e_y e_x$	$S_3^+ B_x \hat{p}_x^2 - \hat{p}_y^2$	$S_4^+ B_x P_{\text{circ}}$
	$j_y=I$	$S_1 B_x$	$S_2 B_x e_x e_y + e_y e_x$	$S_3 B_x \hat{p}_x^2 - \hat{p}_y^2$	$S_4 B_x P_{\text{circ}}$
B_{ky}	$j_x=I$	$S_1 B_y$	$S_2 B_y e_x e_y + e_y e_x$	$S_3 B_y \hat{p}_x^2 - \hat{p}_y^2$	$S_4 B_y P_{\text{circ}}$
	$j_y=I$	$S_1^+ B_y$	$S_2^+ B_y e_x e_y + e_y e_x$	$S_3^+ B_y \hat{p}_x^2 - \hat{p}_y^2$	$S_4^+ B_y P_{\text{circ}}$

TABLE III: Contribution of the different terms of Eqs. (4) and Eqs. (5) to the current at different magnetic field orientations. The two left columns give the magnetic field and the current, respectively.

g is the electron g -factor, μ_B is the Bohr magneton, and E is the average electron energy. The light absorption leads to a non-equilibrium symmetrical distribution of electrons within each spin branch with the average energy different from that in equilibrium. Taking into account the gyrotropic symmetry of the QW, the matrix element for scattering $k; s_x \rightarrow k^0; s_x$ of an electron by a phonon can be presented in the form $M(k^0; s_x; k; s_x) = P + s_x \sum_i^P R_{xi}(k_i^0 + k_i)$, where $P; R_{xi}$ ($i = 1; 2$) as functions of the involved wave vectors have the same parities. Thus, the ratio of antisymmetric to symmetric parts of the scattering probability rate $W_{k^0; s_x; k; s_x}$ is given by $W^{(-)} = W^{(+)} - \sum_i^P R_{xi}(k_i^0 + k_i) = P$. Since the antisymmetric component of the electron distribution function decays within the momentum relaxation time τ_p , one can write for the photocurrent

$$j_i = eN \frac{g \mu_B B_x}{E} W^{(+)} \frac{R_{xi}(k_i^0 + k_i)}{P} \left[\tau_p(k^0) \frac{\hbar k_i^0}{m} - \tau_p(k) \frac{\hbar k_i}{m} \right] \sum_{\#}^+ e_p \frac{R_{xi} g \mu_B B_x}{\hbar P E} I; \quad (6)$$

where e is the electron charge, m is the electron effective mass, $\sum_{\#}^+$ is the fraction of the energy flux absorbed in the QW due to all possible indirect optical transitions, and the angle brackets mean averaging over the electron energy distribution. While deriving Eq. (6)

we took into account the balance of energy:

$$\sum_{k^0k} (E_k - E_{k^0}) W_{k^0k} = I ;$$

where $E_k = \hbar^2 k^2 / 2m$. The contributions to the current from electrons in the branches $s_x = \pm 1/2$ are of opposite sign. However, they do not compensate each other because of the magnetic field induced selective occupation of the branches.

The next mechanism to be considered is based on the asymmetry of spin-flip processes and represents in fact the spin-galvanic effect described by

$$j_i = Q_{ij} (S_j - S_j^0) ; \quad (7)$$

where S is the average electron spin and S^0 is its equilibrium value governed by the ratio $g_B B = E$. The observation of the spin-galvanic effect [14] was carried out under conditions where S^0 was negligible. Then the spin-galvanic current is generated as a result of the spin relaxation which tends to depress the polarization. The same is relevant to the helicity-dependent photocurrent described by the coefficients b_i in Eq. (1). A possible contribution of the spin-galvanic effect to the polarization-independent photocurrent can be interpreted as a light-induced depolarization of the electronic spins followed by the spin relaxation tending to restore the polarization to S^0 . As well as in [14] the asymmetry of spin-flip processes can be related to the k -linear terms in the electron effective Hamiltonian, $H_{BIA} = (b_x k_x + b_y k_y) + (s_{IA} k_x - s_{IA} k_y)$, where the coefficients b_{BIA} and s_{IA} represent the bulk- and structure-inversion asymmetry. Applying the same reasons as in [14] one can estimate the spin-galvanic contribution to the magneto-gyrotropic photocurrent as

$$j = e_p \frac{g_B B_x}{\hbar} \frac{I}{E} \frac{1}{\hbar \tau} ; \quad (8)$$

Here e_p is a factor describing the depolarization of electron spin under photoexcitation followed by energy relaxation. It can be estimated as $e_p = \tau_s / \tau$, where τ is the time of electron energy relaxation governed mainly by electron-electron collisions, and τ_s is the spin relaxation time. Assuming the times to be $\tau = 10^{-13}$ s and $\tau_s = 10^{-10}$ s for the room temperature, the factor e_p can be estimated as 10^{-3} .

Finally, the diamagnetic mechanism is related to spin-independent magnetic field induced k -linear terms, $(B_x k_y - B_y k_x)$, in the electron Hamiltonian, where $B = (eh/c m) z$ and $z = \hbar e / j_z j_i$ is the center of mass of the electron envelope function in the i -th subband [15].

In an asymmetrical QW, z are nonzero and the subband dispersion is given by parabolas with their minima (or maxima in case of the valence band) shifted from the origin $k_x = k_y = 0$ by values proportional to the in-plane magnetic field. One can show that the diamagnetic mechanism contributes to the photocurrent under indirect intra-subband optical transitions only if the indirect transition involves intermediate states in other bands or subbands, $n \neq e1$. Then, the magneto-gyrotropic photocurrent is estimated as

$$j_y = e_p \frac{B_x}{h} \frac{I}{h\nu} \beta^0; \quad (9)$$

where β^0 is a linear combination of the constants β_{e1} and β_{int} in the subband $e1$ and intermediate band. For intermediate states in the valence band, the parameter β^0 is of the order of $(h\nu - E_g)^3$, and, for intermediate states in the next conduction subband $e2$, one has $\beta^0 \sim (h\nu - E_{21})^3$, where E_g is the band gap, and E_{21} is the $e2-e1$ energy spacing.

It is reasonable to expect the ratios $R_{xx} = P$ and $R_{xy} = P$ to be of order of $\beta_{IA} = E$ and $\beta_{SIA} = E$, respectively. The ratio $\beta_{SIA} =$ can be obtained by using the equation for β_{SIA} derived in Ref. [16]. It follows then that, because of the small parameters β and β^0 , it is the first mechanism that is responsible for the magneto-gyrotropic photocurrent induced in InAs/AlGaAs QWs under indirect absorption of the far-infrared radiation.

SUMMARY

In conclusion, it has been shown that in gyrotropic systems the application of an external magnetic field induces in addition to the helicity-sensitive spin-galvanic current a light polarization independent current which we attribute to the magneto-gyrotropic effect. Three different microscopic mechanisms that may contribute to this effect have been considered. Under steady-state optical excitation, the role of each mechanism in the magneto-gyrotropic photocurrent is established through theoretical estimation. However, the three contributions can be separated experimentally in time-resolved measurements. Indeed, after the removal of light or under ultra-short pulsed photoexcitation the magneto-gyrotropic current should decay, for the mechanisms considered above, within the energy (τ), spin (τ_s) and momentum (τ_p) relaxation times, respectively. A photogalvanic detection of the nuclear spin resonance could be another evidence for spin-related mechanisms of the photocurrent.

ACKNOWLEDGEMENTS

The high quality quantum wells were kindly provided by J. De Boeck and G. Borghs from IMEC Belgium. We thank L. E. Golub for helpful discussion.

-
- [1] E.L. Ivchenko and G.E. Pikus, *Pis'ma Zh. Eksp. Teor. Fiz.* 27, 640 (1978) [*JETP Lett.* 27, 604 (1978)].
 - [2] V.I. Belinicher, *Phys. Lett. A* 66, 213 (1978).
 - [3] E.L. Ivchenko, *Usp. Fiz. Nauk* 45, 1461 (2002) [*Phys. Usp.* 45, 1299 (2002)].
 - [4] S.D. Ganichev and W. Prettl, *J. Phys.: Condens. Matter* 15, 935 (2003).
 - [5] E.L. Ivchenko and G.E. Pikus, *Izv. Akad. Nauk SSSR (ser. z.)* 47, 2369 (1983) [*Bull. Acad. Sci. USSR, Phys. Ser.*, 47, 81 (1983)].
 - [6] L.I. Magarill, *Fiz. Tverd. Tela* 32, 3558 (1990) [*Sov. Phys. Solid State* 32, 2064 (1990)].
 - [7] A.A. Gorbatsovich, V.V. Kapaev, and Yu.V. Kopaev, *Pis'ma Zh. Eksp. Teor. Fiz.* 57, 565 (1993) [*JETP Lett.* 57, 580 (1993)].
 - [8] O.V. Kibis, *Physica E* 12, 741 (2002).
 - [9] E.L. Ivchenko and B. Spivak, *Phys. Rev. B* 66, 155404 (2002).
 - [10] A.P. Dmitriev, S.A. Emel'yanov, S.V. Ivanov, P.S. Kop'ev, Ya.V. Terent'ev, and I.D. Yaroshetskii, *Pis'ma Zh. Eksp. Teor. Fiz.* 54, 279 (1991) [*JETP Lett.* 54, (1991)].
 - [11] Yu.A. Alekshchenko, I.D. Voronova, S.P. Grishchikina, V.V. Kapaev, Yu.V. Kopaev, I.V. Kucherenko, V.I. Kadushkin, and S.I. Fomichev, *Pis'ma Zh. Eksp. Teor. Fiz.* 58, 377 (1993) [*JETP Lett.* 58, (1993)].
 - [12] I.V. Kucherenko, L.K. Vodopyanov, and V.I. Kadushkin, *Fiz. Tekh. Poluprovodn.* 31, 872 (1997) [*Semiconductors* 31, 740 (1997)].
 - [13] S.D. Ganichev, *Physica B* 273-274, 737 (1999).
 - [14] S.D. Ganichev, E.L. Ivchenko, V.V. Bel'kov, S.A. Tarasenko, M. Sollinger, D. Weiss, W. Wegscheider, and W. Prettl, *Nature (London)* 417, 153 (2002).
 - [15] T. Ando, A.B. Fowler, and F. Stem, *Rev. Mod. Phys.* 54, 437 (1982).
 - [16] P. Pfeiffer and W. Zawadzki, *Phys. Rev. B* 59, 5312 (1999).